Chapter

Signal Processing for Estimating the Time of Arrival and Amplitude of Nonlinear Underwater Acoustic Waves

María Campo-Valera, Dídac Diego-Tortosa and Rafael Asorey-Cacheda

Abstract

In acoustic environments, many problems arise due to intermodulation distortions that disturb both the timing and amplitude details, and traditional detection methods often do not work well for long-distance communications. This chapter presents an analysis of methods applied to the processing of nonlinear acoustic signals, by means of two approaches, (i) the estimation of the time of arrival (ToA) and (ii) that of the amplitude, two key aspects that usually receive little attention in the literature for this type of signal. This chapter is focused on the nonlinear signals generated by sine-type and sine-sweep modulations, which are characterized by the appearance of low-frequency components due to intermodulation phenomena. These components have a narrow directivity and a high propagation capacity, which is advantageous for long distance transmission and detection applications. Three methods for the ToA estimation are evaluated: threshold, power variance, and cross-correlation. In the amplitude analysis, techniques in the time domain, in the frequency domain, and cross-correlation method are applied. The proposed approaches are validated by a proof of concept with experimental nonlinear signals, demonstrating their robustness, accuracy, and applicability in real scenarios of acoustic propagation.

Keywords: acoustic signal processing, time of arrival estimation, amplitude estimation, underwater acoustics, nonlinear effect

1. Introduction

Underwater acoustic communications represent a highly relevant area of research due to its ability to enable signal interaction in complex underwater environments. Their application is crucial in sectors such as marine ecosystem monitoring [1, 2], maritime traffic management [3], autonomous navigation, and defense and security operations [4]. However, underwater acoustic systems face significant challenges due to the nature of acoustic wave propagation in the marine environment. These challenges include attenuation, background noise and, most importantly, multipath

effects, which introduce significant interference and distortion into the received signals. These factors severely degrade the quality and reliability of acoustic transmission, limiting the effectiveness of underwater communication systems.

To overcome these limitations, acoustic signal processing techniques have been developed based on the nonlinear propagation phenomenon known as the parametric effect. This effect was first described theoretically in the 1960s by Westervelt [5] and later by Berktay, who developed a simplified formulation known as Berktay's approximation [6], which is particularly useful for underwater applications.

The parametric effect is produced by the propagation of high-frequency (primary frequencies) at high acoustic intensity. The nonlinear interaction between these waves, along with others, produces low-frequency components (secondary frequency) that were not originally present in the emitted signal. This secondary signal is characterized by a narrow directivity, more specific of high frequencies, which mitigates multipath effects and improves communication quality.

The analysis of underwater acoustic signals has emerged as a crucial area for various applications, such as sound source localization and acoustic environment characterization [7]. In particular, time of arrival (ToA) estimation is presented as an essential tool for accurate source position determination, especially in complex acoustic conditions. Traditionally, ToA and time difference of arrival (TDoA)-based methods have been used to address these challenges. A recent study compared the performance of these approaches in underwater environments with multipath propagation, using a ray-tracing-based propagation model and Bernoulli filters to mitigate adverse effects. The results showed that the choice between ToA and TDoA depends on the specific environmental conditions and application requirements [8].

With the advancement of deep learning techniques, innovative methods for ToA and direction of arrival (DoA) estimation have been developed. For example, a convolutional recurrent neural network (CRNN) that combines convolutional layers for feature extraction and recurrent layers for modeling temporal information has been proposed to improve the accuracy of DoA estimation in complex underwater environments [9].

In addition, denoising algorithms have been explored to improve the quality of underwater acoustic signals, which indirectly benefits ToA estimation by reducing interference from ambient noise. A comprehensive review of these algorithms highlights the importance of developing more robust and adaptive denoising techniques to address the unique challenges of the underwater environment [10].

Knowing the ToA of a received signal enables a more comprehensive analysis of its amplitude. Accurately parameterizing the amplitude of the received signal opens up possibilities for various studies, such as those on the propagation of acoustic signals in the environment, the assessment of noise pollution in surrounding areas, and the characterization of the acoustic properties of the medium, among others.

This chapter focuses on the treatment and analysis of nonlinear acoustic signals, more specifically the phenomenon of the parametric effect. This phenomenon must be carefully analyzed in order to obtain an accurate estimate of the relevant parameters, such as ToA and amplitude. Despite its relevance, the specific analysis of this type of nonlinear signals in underwater environments has been scarcely addressed in the scientific literature, with the authors of this chapter being pioneers in proposing a detailed study framework in [11].

A methodological approach divided into two main stages is proposed. The first approach focuses on the estimation of the ToA using three methods: threshold, power variation (Pvar), and cross-correlation. The selection of the optimal method depends

on the propagation environment conditions, signal intensity, and the system's computational cost, as each method offers specific advantages depending on the noise level, the complexity of the acoustic channel, and the processing time requirements.

Once the ToA has been detected, the second approach is applied, which focuses on estimating the signal amplitude. This is done by time and frequency domain analysis, complemented by the use of the cross-correlation method (also used in the time domain). The time domain analysis allows the characterization of the evolution of the signal, providing critical information on the propagation effects. Spectral analysis, based on the Fourier transform, identifies the frequency components of the signal and evaluates their contribution to the observed nonlinear behavior. The cross-correlation method not only contributes to the accurate estimation of the ToA, but also enables the evaluation of the similarity between the expected and received signals, even under adverse conditions with a low signal-to-noise ratio (SNR), thus improving the reliability of the acoustic detection and characterization process.

The use of sine-type and sine-sweep type signals, together with filtering techniques, is key to separating the relevant components from the noise and improving the quality of the ToA estimation. By comparing different processing methods and applying experimental measurements, the aim is not only to characterize the behavior of underwater nonlinear acoustic signals but also to validate the estimation techniques in real-world scenarios where acoustic and environmental conditions can vary significantly.

This integrative approach is advancing the understanding and improvement of underwater communication and sensing technologies, opening new perspectives for applications ranging from ocean exploration to aquatic security communications.

2. Background for nonlinear signals

The parametric underwater acoustic communications take advantage of the nonlinear effects generated in the underwater channel for efficient data transmission. These communications are based on the use of bi-frequency signals, which allow for generating nonlinear interactions that facilitate the propagation of the signal in the medium. A bi-frequency signal of pressure $p'(0,t)$ can be expressed as follows:

$$p'(0,t) = A_a \sin(\omega_a t) + A_b \sin(\omega_b t), \tag{1}$$

where ω_a and ω_b are the high primary frequencies, which should be close to each other, while A_a and A_b are the amplitudes of these frequencies, and they should increase as the distance between the frequencies grows.

When a medium such as water is excited by a bi-frequency signal, as described in Eq. (1), interactions between frequencies are generated due to nonlinear channel effects. These interactions give rise to secondary waves whose frequency corresponds to linear combinations of the primary frequencies, specifically the sums and differences of these, a phenomenon known as beat frequencies. In addition, the medium has dissipative effects that attenuate the higher-frequency waves, causing them to disappear with distance before the produced nonlinear low frequencies. As the signal propagates over long distances from the source, the predominant signal is the one defined as the difference ω_d, the difference between the primary frequencies: $\omega_d = \omega_a - \omega_b$.

This phenomenon is especially important because ω_d, the low-frequency signal, suffers less attenuation and can propagate over longer distances, allowing more efficient communication. This effect, known as the *parametric effect*, not only generates

low-frequency signals but also produces narrower radiation patterns, a characteristic of higher primary frequencies [12, 13]. Moreover, a remarkable property of this effect is that it facilitates reliable signal detection and demodulation, which improves the quality and reliability of transmission in underwater environments.

Assuming that $A_a = A_b = A_c/2$, Eq. (1) can be rewritten as follows:

$$p'(0,t) = A_c \cos(\omega_m t)\sin(\omega_c t) = \frac{A_c}{2}\sin\left(\underbrace{(\omega_c + \omega_m)}_{\omega_a} t\right) + \frac{A_c}{2}\sin\left(\underbrace{(\omega_c - \omega_m)}_{\omega_b} t\right), \quad (2)$$

where ω_m is the frequency of the modulating signal (low-frequency signal), ω_c is the frequency of the carrier signal (high primary frequency), and A_c is the amplitude of the carrier signal. In this context, if the envelope $E(t)$ is a harmonic signal, i.e., $E(t) = \sin(\omega_m t)$, the excitation will be reduced to a bi-frequency signal. As a result, the difference frequency $\omega_d = 2\omega_m$ will be twice the frequency of the modulating signal.

Thus, for any signal containing an envelope, the demodulation is related to the second derivative of the time-square envelope, $E^2(t)$, as shown in Eq. (3). This process is fundamental for obtaining the parametric signal, which is defined as p_{param}, and is the way in which the modulated signal can be efficiently recovered from frequency modulation and nonlinear interaction in the channel.

$$p_{param} \sim \frac{\partial^2 E^2(t)}{\partial t^2} \quad (3)$$

The process of obtaining underwater acoustic parametric signals begins with a modulated signal, as shown in Eq. (2). A parametric signal must be designed in such a way that it can be decoded even under the effects of nonlinear propagation [14].

In this chapter, the parametric effect is presented through two different types of amplitude modulated (AM) signals: a sine-type signal and a sine-sweep signal. In the first case, ω_m will remain constant (tone), while in the second case, ω_m will vary. The $E(t)$ of the wideband (sine-sweep) signal is defined as presented in Eq. (4):

$$E(t) = \sin\left(\left(\frac{|\omega_{m2} - \omega_{m1}|}{\tau} t + \omega_{m1}\right) t\right), \quad (4)$$

where ω_{m1} is the initial frequency of the sine-sweep, ω_{m2} is the final frequency of the sine-sweep, τ is the total duration of the sine sweep, and t is time. Define $\omega_d = |\omega_{m2} - \omega_{m1}|$.

The profile of the parametric signal in Eq. (3) can be obtained as:

$$p_{param} \sim 4\frac{\omega_d}{\tau}\sin\left(2\left(\frac{\omega_d}{\tau} t + \omega_{m1}\right)\right) + 2\left(\frac{2\omega_d}{\tau} t + \omega_{m1}\right)^2 \cos\left(2\left(\frac{\omega_d}{\tau} t + \omega_{m1}\right)\right) \quad (5)$$

In Eq. (5), the parametric signal has a frequency twice that of the modulating frequency, and an initial amplitude of zero that increases proportionally to t^2. In this manner, the modulation scheme described in Eq. (4), along with the theories of Westervelt [5] and Berktay [6], models the parametric transmission. For a more detailed analysis of these developments, see [15].

3. Experimental setup and measured signals

To demonstrate the generation of the parametric effect in the measured signals, the experimental setup used consists of a cylindrical tank with a capacity of approximately 19 m^3. The acoustic signal transmitter used was the Airmar P19, which has an emission sensitivity of 167 dB (re 1 μPa/V at 1 m) and a resonance frequency of 200 kHz, making it a very effective device for generating signals in the desired frequency range (carrier frequency, f_c, of 200 kHz).

The used receiver was the hydrophone Reson TC4040, which has a receiver sensitivity of −206 dB (re 1 V/μPa at 1 m) from 2 kHz to 75 kHz. The choice of this hydrophone is particularly suitable for the analysis of the parametric frequencies measurements in the experiments, which are centered in the range from 2 kHz to 20 kHz, making it an ideal choice for obtaining accurate results.

The distance between the transducers, crucial for the analysis of acoustic wave propagation, was set at 42 cm, ensuring the maximum separation without interfering with the recordings due to reflections while considering the characteristics of the tank.

Figure 1 illustrates in detail the experimental setup and the arrangement of the necessary connections for the calibration of the equipment. The E&I 1040 L amplifier, combined with a data generation and acquisition system consisting of a National Instruments PXI-1073 chassis, a PXIe-5433 waveform generator card, and a PXIe-5122 oscilloscope, is operated and controlled via a laptop using the NI PXI ExpressCard-8360. Additionally, to ensure proper signal acquisition, a Testec TT-HV-400 ×100 attenuating probe was incorporated, which allows attenuation of the signal at the amplifier output, facilitating its subsequent recording by the PXI system.

In real-world environments, where the receiver and transmitter operate independently, synchronizing both devices using a common reference, such as the global positioning system (GPS), becomes a critical factor for making accurate ToA measurements. However, in cases where the primary goal is the detection of signals containing information (such as bit strings), strict synchronization may not be as crucial. In such cases, the detected signals can be recorded according to the receiver system's internal clock, whether using universal time coordinated (UTC) or not.

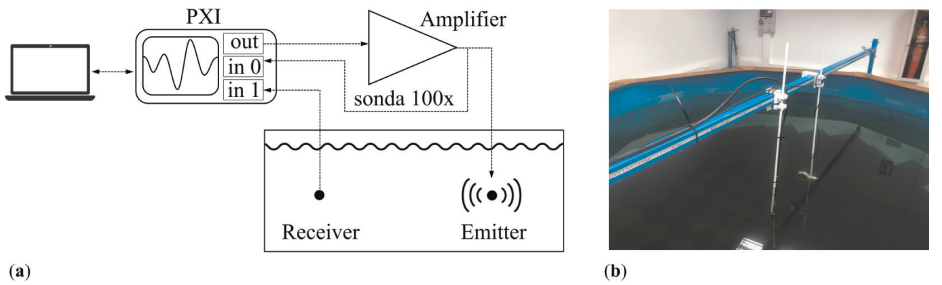

Figure 1.
Experimental setup for measuring nonlinear signals. (a) Equipment used in the experiment, including the computer, amplifier, and PXI system, which allow the generation and acquisition of acoustic signals. (b) View of the tank and the transducers placed at a distance of ∼ 42 cm, setup to study the propagation of acoustic waves.

4. Time of arrival estimation of acoustic signals

Once the measurements have been taken, each recorded signal must be analyzed to examine the parameters of interest. In this case, the recorded waveform will consist of background noise and the signal emitted by the transducer, which will appear at a ToA corresponding to the time of flight (ToF) between the emitter and the receiver. This section will describe three different methods for estimating the ToA for the desired signal.

4.1 Threshold method

The threshold method consists of determining the point at which the signal surpasses a predefined amplitude level (threshold level). This technique demands a good SNR (more than 30 dB) and a detailed evaluation of the emitted signal to set an appropriate threshold in the receiver point, which is defined as the minimum received signal level. Furthermore, this method depends on the time transition of the received signal; that is, if it takes longer to reach a noticeable level relative to the background noise, the calculation of the ToA may not be very accurate. This issue is typically linked to the resonance effect of the transmitter and/or receiver at the frequencies of the emitted signal. In many instances, filtering is essential to capture the signal of interest with greater precision. However, it is important to account for the delay it may introduce to the signal, as this will need to be corrected for an accurate ToA calculation. An example of the threshold method application is shown in **Figure 2**.

4.2 Pvar method (Pvar)

The Pvar method has similar requirements to the threshold method regarding the SNR and the time transition of the received signal and may also require efficient signal filtering. This method includes two variants: "cumulative Pvar" ($Pvar_{cum}$) and "saw Pvar" ($Pvar_{saw}$).

To implement the mathematical formulas $Pvar_{cum}$ and $Pvar_{saw}$, a custom analysis function was created. This function processes the signal using the Pvar-transform

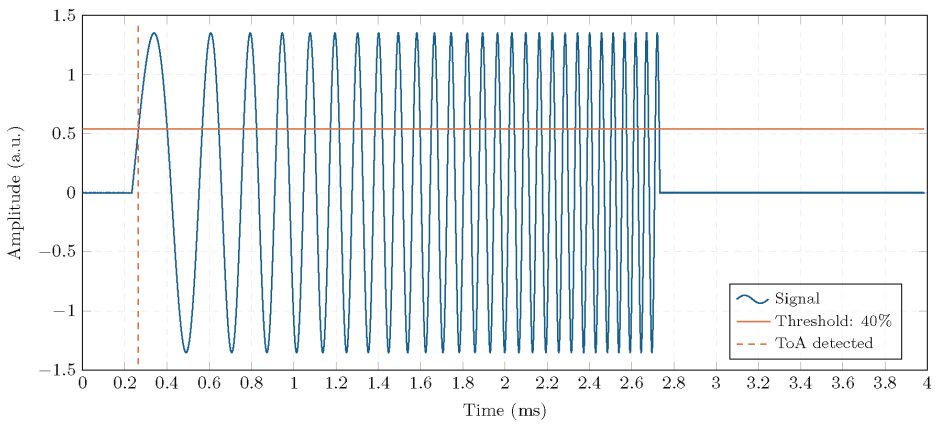

Figure 2.
An example of ToA estimation using the threshold method is shown for a theoretical sine-sweep type signal with a SNR of 90 dB. The threshold level is set at 40% of the signal's maximum amplitude. The estimated ToA is 0.26 ms.

within a defined time window, identifying shifts in the slope of the transformed signal.

The point of intersection between the two first slopes is then computed, which corresponds to the estimated ToA.

4.2.1 Cumulative power variation ($Pvar_{cum}$)

The $Pvar_{cum}$ method computes the cumulative sum of the absolute values of the recorded waveform's amplitude, as represented in Eq. (6) [16]. This approach highlights an increasing trend in the values, with a distinct change in slope when the target signal emerges. By modifying a specific power factor, the slope's steepness can be enhanced, facilitating the identification of the ToA.

$$Pvar_{cum}[n] = \frac{\sum_{i=1}^{n} x_i^k}{\sum x[n]^k}, \tag{6}$$

where k represents the power factor to which each data point x_i is raised, and n represents the total number of data points in the dataset. An example of this method is illustrated in **Figure 3** (orange color). In this case, k is 2.

4.2.2 Saw power variation ($Pvar_{saw}$)

The $Pvar_{saw}$ method involves subtracting the mean value of the recorded waveform from $Pvar_{cum}$ (Eq. (6)), generating a sawtooth-like signal that compensates for background noise contributions, which may reduce the need for extra filtering. The ToA of the signal is identified by the first change in slope observed in $Pvar_{saw}$, as depicted in **Figure 3** (yellow color).

$Pvar_{saw}$ can be obtained as follows [17]:

$$Pvar_{saw}[n] = Pvar_{cum}[n] - Noise[n] \tag{7}$$

$$Noise[n] = a \cdot tn + b, \tag{8}$$

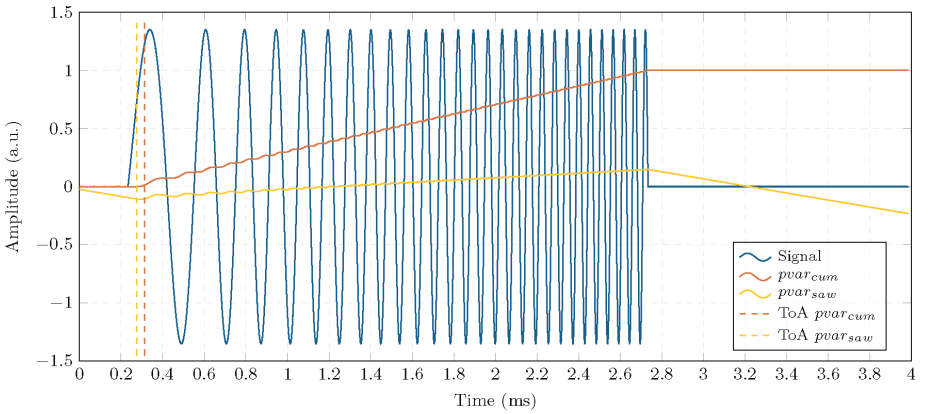

Figure 3.
An example of ToA estimation using the Pvar method is shwon for a theoretical sine-sweep type signal with a SNR of 90 dB. The orange and yellow lines represent the estimated ToA using $Pvar_{cum}$ and $Pvar_{saw}$, respectively. The ToA estimated by $Pvar_{cum}$ is 0.31 ms, while $Pvar_{saw}$ yields an estimate of 0.27 ms.

where, in Eq. (8), a and b represents the coefficients resulting from the linear fit of $Pvar_{cum}$, and $t[n]$ represents the time vector of the discrete-mode signal.

4.3 Cross-correlation method

The cross-correlation method analyzes the similarity between the transmitted signal and the recorded waveform by generating the correlation signal [18]. The amplitude peaks will increase as the two signals align, providing the ToA at its maximum peak. Unlike the previously mentioned methods, this approach is much more effective in noisy conditions without the need for filtering, and yields better results with sine-sweep type signals, since they contain more frequency components to compare.

$$r_{xy}[l] = \sum_{i=1}^{N} x[n]y[n+l] \tag{9}$$

In Eq. (9), $x[n]$ y $y[n]$ denote the signals digitized by the transmitting transducer and the hydrophone, respectively. In this case, $l = 1, 2, \ldots, N$ represents the number of samples by which y is delayed relative to x.

An example of the cross-correlation method application is shown in **Figure 4**.

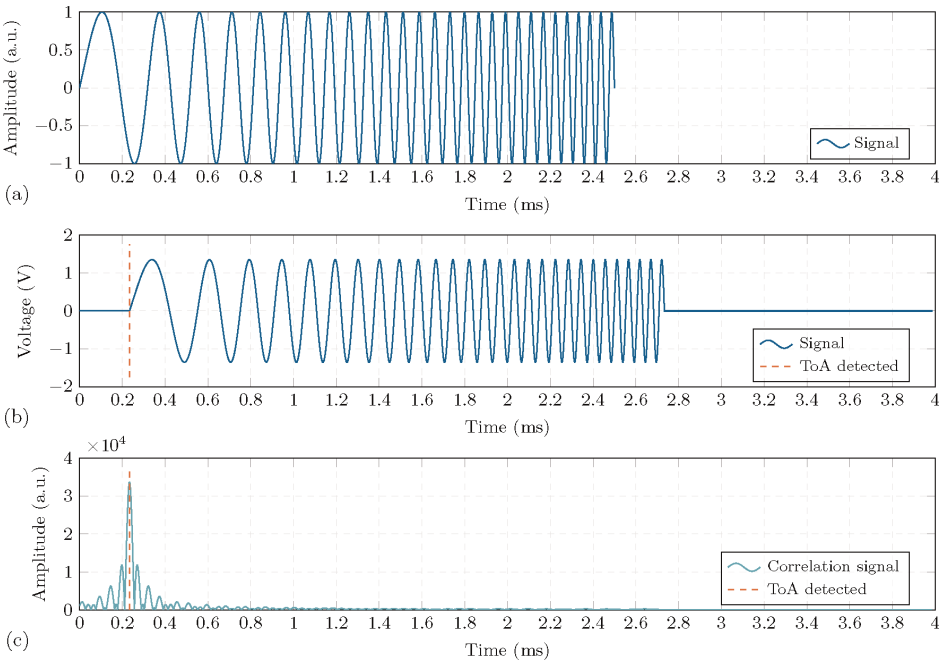

Figure 4.
An example of ToA estimation using the cross-correlation method for a theoretical sine-sweep type signal with an SNR of 90 dB. It shows in (a) the transmitted signal. (b) The received signal. (c) The cross-correlation waveform between them, with a clearly defined peak in the ToA of 0.23 ms.

5. Amplitude estimation of the acoustic signals

Once the ToA is estimated, its amplitude can be studied. To achieve this, three different techniques are analyzed: the time domain, the frequency domain, and the cross-correlation method (also used in the time domain). All these techniques provide the same value for an ideal signal (free of noise). However, depending on the experimental setup and background noise, differences may arise between them, which should be considered. Each technique is described in detail below, highlighting the specific information it provides about the received signal, which is measured in voltage V in this study.

5.1 Amplitude in the time domain

Time domain refers to the detailed description of the behavior of a signal with respect to time, which is the fundamental domain inherent to all acoustic signals. Time is the most basic and universal variable used to characterize the evolution of any dynamic phenomenon. In the case of acoustic signals, its temporal analysis allows for the study of their propagation, attenuation, and variability along their trajectory. Although this parameterization is the most basic, it is crucial for extracting essential information from the signal, such as its amplitude, frequency, and duration, which are necessary for a wide range of applications in acoustic signal processing.

In the discrete-time domain, the signal is observed only at specific moments along the time axis. This means that the signal is represented by discrete values taken at regular intervals. The amplitudes of these values are quantized, meaning they cannot take any continuous real value, but are limited to those defined by the resolution of the quantization, which is determined by the bit depth of the sampling system. This discretization process allows the acoustic signal to be represented in digital form, facilitating its processing with computational tools. The digitalization of the signal involves taking a sequence of N samples at regular intervals, separated by a period $T = 1/f_s$, where f_s is the sampling frequency, a fundamental parameter that must be appropriately selected to capture the characteristics of the signal under study, in accordance with the Nyquist–Shannon theorem, which limits the highest recorded frequency to half of the f_s.

Once the signal has been digitized, it becomes particularly relevant within the context of this study to obtain information about the signal in terms of specific frequencies and/or frequency bands. To extract this information in the time domain, filtering becomes an essential tool. This process is of utmost importance in the analysis of acoustic signals, as it allows for focusing solely on the relevant characteristics of the signal within a determined frequency range, discarding those frequencies outside the range of interest.

In the digital processing of the acoustic signals in this study, filtering primarily serves two functions: (*i*) remove unwanted noise and (*ii*) analyze the signal in specific frequency bands.

In this work, to compare amplitudes between different analysis domains (such as time and frequency domain), the peak value $V_{p,\text{time}}$ is used as a reference parameter. This value provides a measure of the maximum amplitude reached by the signal in the time domain. The choice of the peak value as an amplitude measure is justified by its ability to capture the extreme fluctuations of the signal. For stationary harmonic signals, this peak value can be estimated as [19]:

$$V_{p,\text{time}}\{x[n]\} = V_{rms,\text{time}}\{x[n]\} \cdot \sqrt{2} = \sqrt{\frac{1}{N}\sum_{i=1}^{N}(x_i - \overline{x})^2} \cdot \sqrt{2}, \tag{10}$$

where $x[n]$ is the discretely sampled version of the continuous signal, x_i is the i-th sample of the signal, $\overline{x}$ is the mean (DC component) of the signal, and N is the total number of samples.

5.2 Amplitude in the frequency domain

The Fourier transform $X(f)$ converts a signal from the time domain to the frequency domain. It is a widely used technique for analyzing stationary signals, providing the spectral characteristics of one or more frequencies without altering their content. This representation is fundamental for signal analysis because it allows the study of how energy is distributed across different frequencies.

In the Fourier transform, the signal is interpreted as a superposition of sine waves with periodic amplitude, constant frequency, and phase, that is, harmonic components. The mathematical relationship that describes how the signal transforms from the time domain $x(t)$ to the frequency domain $X(f)$ explains how each frequency component contributes to the overall behavior of the signal in time and is given by the following expressions [20, 21]:

$$X(f) = \frac{1}{\sqrt{2\pi}}\int_{-\infty}^{\infty} x(t) \cdot e^{-j2\pi ft} dt \Leftrightarrow x(t) = \frac{1}{\sqrt{2\pi}}\int_{-\infty}^{\infty} X(f) \cdot e^{+j2\pi ft} df \tag{11}$$

The amplitude of the frequency method is determined by analyzing the energy of the signal within a specified frequency range, defined by f_{low} and f_{high} frequencies. Initially, the signal is transformed from the time domain to the frequency domain using the fast Fourier transform (FFT) which provides information about the frequency components of the signal [21]. Then, the amplitude at a specific frequency is calculated based on the corresponding value in the frequency spectrum. The amplitudes across the specified frequency range are summed to yield a total amplitude value, $V_{p,\text{freq}}$.

$$V_{p,\text{freq}} = [X(f)]_{f_{\text{low}} \le f \le f_{\text{high}}}, \tag{12}$$

where f_{low} and f_{high} are the lower and upper frequency ranges to be analyzed.

5.3 Amplitude in the cross-correlation method

In cross-correlation, the resulting waveform reflects the degree of similarity between two signals: the reference signal and the recorded signal. This process produces a time domain representation in which the amplitude of the peaks provides a characteristic or identification of the signal, showing where these peaks occur in relation to the time origin of the transmitted signal. It is possible to estimate the maximum voltage amplitude, $V_{p,\text{corr}}$, of the received signal using the following expression [22]:

$$V_{p,\text{corr}}[y_{rec}] = \frac{2V_{\text{max,corr}}}{V_{p,\text{send}} \cdot N_{\text{send}}}, \tag{13}$$

where $V_{p,\text{send}}$ is the amplitude of the signal, N_{send} is the number of samples in the emitted signal, and $V_{\text{max,corr}}$ is the maximum value of the correlation waveform between the reference signal and the recorded signal, occurring at the instant of detection.

6. Implementation using the proposed methods

Once the methodology for estimating the ToA and the corresponding signal amplitude is presented, this section analyzes two types of experimental parametric (nonlinear) acoustic signals: (*i*) a sine-type signal and (*ii*) a sine-sweep type signal. For each signal type, five measurements were recorded to ensure repeatability and robustness in the analysis.

As mentioned above, the distance between the transmitter and receiver in the experimental setup is 42 cm. Assuming a sound propagation speed of 1500 m/s in water, the received signal is expected to appear approximately 0.28 ms after the start of the measurement. This value is used as a reference for the experimental ToA estimations.

The transmitted signals have a carrier frequency, f_c, of 200 kHz and are recorded with a sampling frequency, f_s, at 20 MHz. The sine-type signal is created with a modulating frequency, f_m, of 15 kHz, and a duration of 500 μs, which is expected to produce a parametric signal at twice the frequency, i.e., 30 kHz. For the sine-sweep signal, the frequency range is 2 kHz to 20 kHz (f_{m1} and f_{m2}), so the expected parametric signal is 4 kHz to 40 kHz, with a duration of 1000 μs.

The structure used to implement the proposed approaches, which include (*i*) the estimation of the ToA and (*ii*) the estimation of the amplitude of the signals, is developed as follows: first, the recorded signal (already filtered to distinguish the primary and secondary -nonlinear- frequency components) is presented in the time domain. To visualize its spectral content and validate the presence of the parametric effect, the corresponding spectrograms are shown. Once the parametric effect is confirmed, the ToA of the primary signals is estimated. Subsequently, the amplitude of the primary frequencies is determined in order to complete the analysis of the nonlinear signal amplitude. For the amplitude estimation, the ToA is used to clip the received signal in the time domain before the $V_{p,\text{time}}$ and $V_{p,\text{freq}}$ calculation (see Appendix). This step is essential, and care must be taken to cut and isolate the signal accurately, as these methods are sensitive to noise.

The objective is to implement the proposed methods within a representative scenario, thereby establishing a methodological framework that will serve as a benchmark for future analyses of nonlinear acoustic signals.

6.1 Results of the sine-type signals

Once the sine-type signals were recorded, a detailed study of the appearance of the parametric effect was carried out. **Figure 5** shows a normalized comparison between the primary and secondary signals in the time domain. The raw signal is processed using a third-order Butterworth low-pass filter with a cut-off set to 5% above the frequency of interest ($f_c + f_m$ for the primary signal, and $2 \cdot f_m$ for the secondary signal). The peak amplitudes, V_p, of the primary and secondary frequencies are 33.88 $\pm$ 0.00 mV and 25.56 $\pm$ 2.85 μV, respectively. This corresponds to a difference of 33.86 mV, equivalent to -29.41 dB.

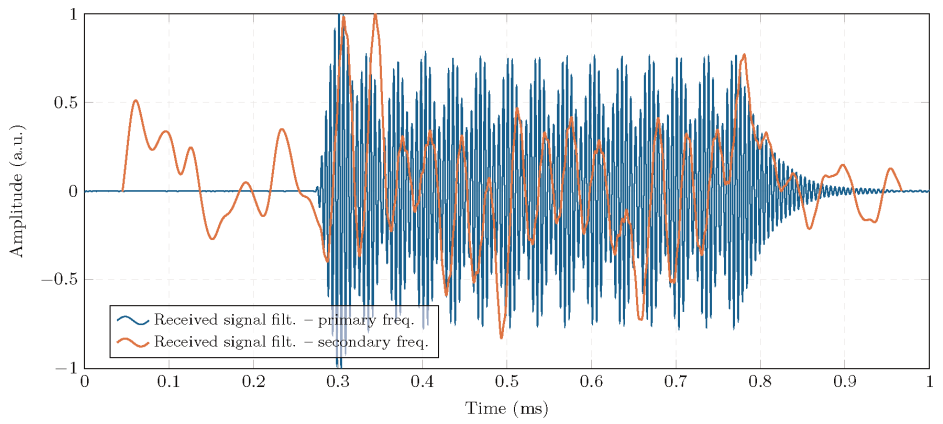

Figure 5.
Received sine-type signal processed through a third-order Butterworth low-pass filter with a cut-off set to 5% above the frequency of interest. The blue signal represents the primary frequency (around f_c) with a $V_p = 33.88$ mV. The orange signal corresponds to the secondary frequency component (twice the f_m) with a $V_p = 25.56$ µV. Both signals have been normalized to their V_p.

Regarding the SNR, there is a significant difference between the primary and secondary frequencies, with values of 68.09 ± 0.72 dB and 11.91 ± 2.06 dB, respectively. Therefore, the ToA was estimated using the primary signal, since, as shown in the figure, the secondary signal exhibits high temporal fluctuations, making accurate ToA estimation unfeasible in the threshold and Pvar methods.

A spectrogram is a powerful tool that displays the frequency components of a signal over time. It can be used to verify the presence of both the primary and secondary frequency components (i.e., the parametric signal) in the recorded data, in accordance with the characteristics described in Section 2.

For proper display, these signals have been decimated by a factor of 25 for the primary frequency and 50 for the secondary frequency using a second-order Chebyshev filter. **Figure 6** show the resulting spectrograms. An NFFT with 128 samples was applied, using a 75% overlap, resulting in a frequency resolution (F_{bin}) of 1 kHz. This configuration yields a time resolution (T_{bin}) of 40µs for the primary signal

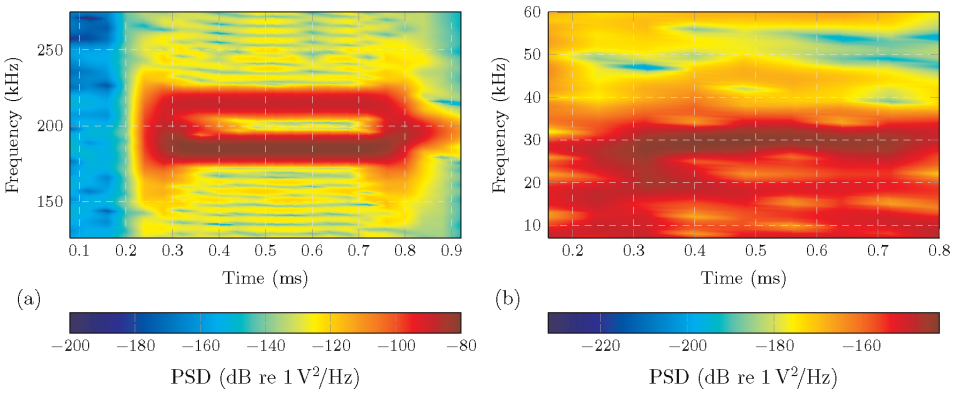

Figure 6.
Spectrogram for the sine-type signal with an NFFT of 128 samples with a 75% overlap and F_{bin} of 1 kHz. (a) The received signal with primary frequency components around the f_c with a T_{bin} of 40 µs. (b) The received signal with a spectral component of the secondary frequency (parametric signal) at 30 kHz with a T_{bin} of 80 µs.

ToA methods	ToA estimation (μs)
Threshold	283.09 ± 0.02
$Pvar_{cum}$	288.51 ± 0.01
$Pvar_{saw}$	288.49 ± 0.01
Cross-correlation	287.37 ± 0.03

Table 1.
Estimation of the ToA of the received sine-type signal by the three methods under analysis of the primary frequency.

and 80 μs for the secondary signal. The minimum valid frequencies (F_{valid}) are 12.5 and 6.25 kHz, respectively, for the primary and secondary signals. A more detailed development of this process can be found in [2].

The first approach proposed in this chapter focuses on the estimation of the ToA for the sine-type signal received and filtered at high frequencies, corresponding to the primary frequency. This choice is justified by the significantly higher SNR of the primary component compared to the secondary one, which enables a more accurate estimation using all the proposed approaches. In this occasion, for the threshold method, a threshold level of 30% over the maximum signal value is used, while for the Pvar method, an order of $k = 2$ is applied.

Table 1 presents the ToA for the threshold method, the Pvar method, and the cross-correlation. In the case of the sine-type signal, it can be seen that the estimated ToA values are consistent in all the methods analyzed.

Once the ToA values are obtained, the amplitudes of the primary frequency are analyzed using the second proposed approach in this chapter: time domain analysis, frequency domain analysis, and the cross-correlation method.

The amplitude of the secondary (parametric) frequency is evaluated using frequency domain analysis and the cross-correlation method. Cross-correlation enables the comparison of the received signals with reference signals, improving the accuracy of amplitude estimation and providing a more robust assessment of their behavior than either time or frequency domain analysis alone. Previous studies, such as those in [11], indicate that amplitude detection in the time domain is unclear due to the low SNR (less than 20 dB), which is why this approach is excluded from the current analysis.

The advantage of the cross-correlation method is that it produces a distinct peak at the location of the received signal, even when applied to the detection of the secondary (parametric, low-frequency) component. The sharpness of this peak may vary, indicating the accuracy of the ToA estimation. However, it also provides a useful indication of the amplitude of the received signal, as shown in **Figure 7**.

Figure 7a shows the transmitted signal correlated with the received signal previously filtered at the primary frequency (blue signal in **Figure 5**). The result is a correlation peak with a detection amplitude of 65.90, shown in **Figure 7b**.

On the other hand, the second derivative of the time-squared envelope of the transmitted signal is shown in **Figure 7c**. This is correlated with the received signal filtered at the secondary frequency (orange signal in **Figure 5**), giving a correlation amplitude of 0.04, as shown in **Figure 7d**.

A summary of the second approach proposed in this chapter, related to the amplitude estimation, for the primary and secondary frequencies is shown in **Table 2**.

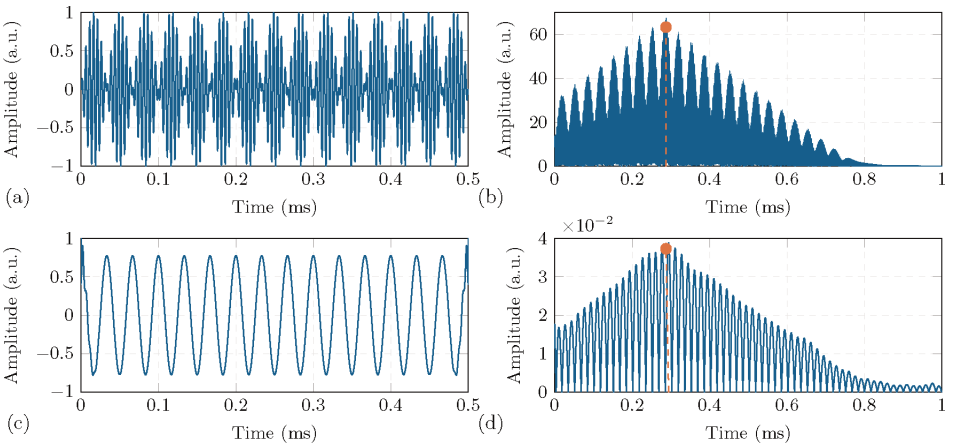

Figure 7.
Cross-correlation of the sine-type signal for the primary and secondary frequencies. (a) Transmitted modulated signal. (b) Cross-correlation between the transmitted modulated signal and the received signal filtered at the primary frequency, with a correlation amplitude of 65.90 in 287.4 µs. (c) Parametric signal corresponding to the second derivative of the time-square envelope of the transmitted signal. (d) Cross-correlation of the parametric signal with the received signal filtered at the secondary frequency, yielding a correlation amplitude of 0.04 in 294.4 µs.

Amp. methods	Estimation of amplitude at primary frequencies (mV)
$V_{p,time}$	20.10 ± 0.00
$V_{p,freq}$	18.28 ± 0.00
$V_{p,corr}$	13.18 ± 0.00
	Estimation of amplitude at secondary frequencies (µV)
$V_{p,freq}$	7.44 ± 0.00
$V_{p,corr}$	7.72 ± 0.46

Table 2.
Amplitude V_p estimation of the received sine-type signal analyzed by time domain, frequency domain, and cross-correlation method, for the primary and secondary frequencies (parametric signal).

6.2 Results of the sine-sweep type signal

As in the previous case, the raw signal is processed using a third-order Butterworth low-pass filter with a cut-off set to 5% above the frequency of interest ($f_c + f_{m2}$ for the primary signal, and $2 \cdot f_{m2}$ for the secondary signal). **Figure 8** shows the normalized comparison of the two signals in the time domain. The peak amplitudes, V_p, of the primary and secondary frequencies are 61.90 ± 0.03 mV and 48.89 ± 2.39 µV, respectively. This corresponds to a difference of 61.82 mV, equivalent to −24.20 dB.

The progressive decrease in the amplitude of the received signal with time can be attributed to the frequency response of the Reson TC4040 hydrophone, whose sensitivity drops significantly after 80 kHz. However, for the parametric frequency range of interest in this study, it is essential to have as flat a sensitivity response as possible, a criterion that this hydrophone adequately satisfies.

In this case, the SNR of the primary frequency is 71.86 ± 1.02 dB, while that of the secondary frequency is 14.73 ± 1.03 dB. As with the sine-type signal, there is a

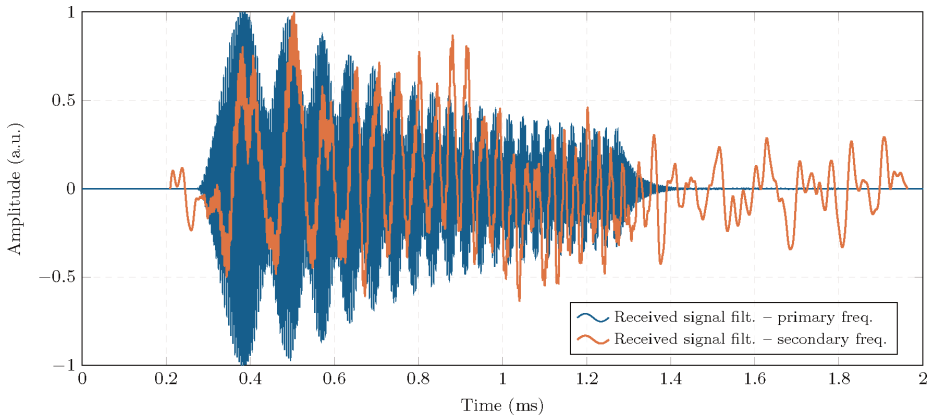

Figure 8.
Received sine-sweep type signal processed through a third-order Butterworth low-pass filter with a cut-off set to 5% above the frequency of interest. The blue signal represents the primary frequency (around f_c) with a $V_p = 61.90$ mV. The orange signal corresponds to the secondary frequency component (twice from f_{m1} to f_{m2}) with a $V_p = 48.89$ µV. Both signals have been normalized to their V_p.

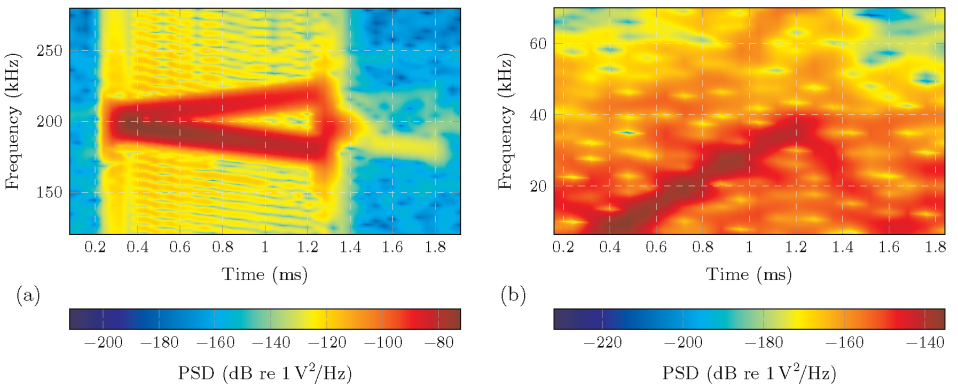

Figure 9.
Spectrogram for the sine-sweep signal with an NFFT of 128 samples with a 75% overlap and F_{bin} of 500 Hz. (a) The received signal with primary frequency components around the f_c with a T_{bin} of 40 µs. (b) The received signal with a spectral component of the secondary frequency (parametric signal) at 4 kHz to 40 kHz with a T_{bin} of 80 µs.

noticeable difference between the two components. Since the primary frequency has a significantly higher SNR, its ToA can be estimated more accurately.

To verify that the parametric effect has been generated in the medium, the sine-sweep type signal is analyzed by a spectrogram with the same NFFT used for the sine-type signal. **Figure 9(a)** shows the content of the primary frequency, around the f_c, while **Figure 9(b)** clearly shows the expected parametric effect, manifested as a frequency between 4 to 40 kHz.

The ToA estimation was performed using the primary received signal. The values corresponding to the proposed methods are summarized in **Table 3**.

As mentioned above, the method that provides the most reliable results is the cross-correlation method, as it demonstrates superior performance under high noise conditions. This time, this effect is more noticeable, as the sine-sweep signal has a longer rise time compared to the sine-type signal.

ToA methods	ToA estimation (μs)
Threshold	313.34 ± 0.02
$Pvar_{cum}$	338.37 ± 0.01
$Pvar_{saw}$	338.36 ± 0.01
Cross-correlation	267.53 ± 0.03

Table 3.
Estimation of the ToA of the received sine-sweep signal by the three methods under analysis of the primary frequency.

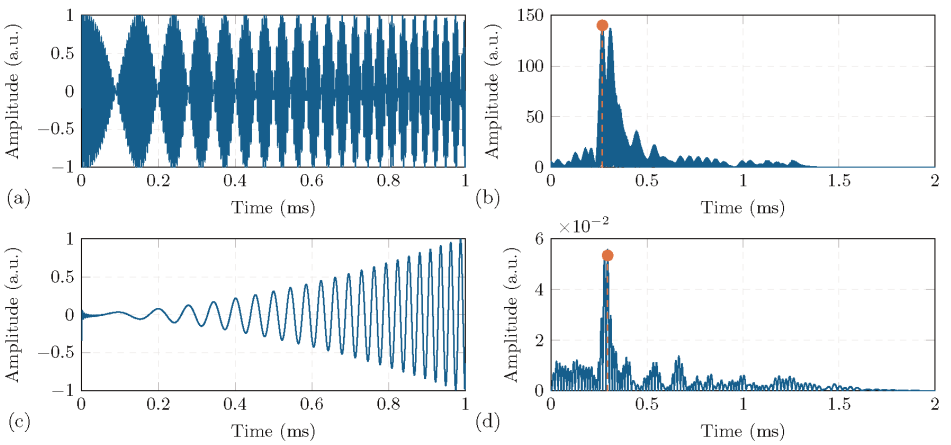

Figure 10.
Cross-correlation of the sine-sweep signal for the primary and secondary frequencies. (a) Transmitted modulated signal. (b) Cross-correlation between the transmitted modulated signal and the received signal filtered at the primary frequency, with a correlation amplitude of 145.71 in 267.55 µs. (c) Parametric signal corresponding to the second derivative of the time-square envelope of the transmitted signal. (d) Cross-correlation of the parametric signal with the received signal filtered at the secondary frequency, yielding a correlation amplitude of ∼ 0.05 in 294.80 µs.

Once the ToA values are determined, the primary frequency amplitudes of the sine-sweep signal are estimated using the second approach proposed in this chapter: time domain, frequency domain, and cross-correlation method.

The secondary frequency amplitude is estimated in the frequency domain and with the cross-correlation method. As in the sine-sweep signal analyzed, the time-domain approach is not considered in the sine-sweep signal.

For the amplitude estimation of the received signal using the cross-correlation method, the results obtained for the primary frequency (high frequency) and the secondary frequency (parametric signal) are presented in **Figure 10**. **Figure 10(a)** shows the sine-sweep transmitted signal correlated with the received signal filtered at high frequencies (**Figure 8**, blue), yielding **Figure 10(b)**. This analysis presents the cross-correlation results with a correlation amplitude value of 145.70 for the primary frequency. On the other hand, **Figure 10(c)** shows the second derivative of the time-squared envelope of the transmitted signal correlated with the received signal filtered at low frequencies (**Figure 8**, orange). The resulting cross-correlation is shown in **Figure 10(d)**, with a correlation amplitude of 0.05 for the secondary frequency.

The correlation peaks in this type of signals are narrower than in a sine-type signal because the sine-sweep has a wider bandwidth. This means that it includes many frequencies, which makes it possible to better locate the exact moment at which the

Amp. methods	Estimation of amplitude at primary frequencies (mV)
$V_{p,time}$	32.59 ± 0.00
$V_{p,freq}$	6.35 ± 0.00
$V_{p,corr}$	14.57 ± 0.00
	Estimation of amplitude at secondary frequencies (μV)
$V_{p,freq}$	3.14 ± 0.00
$V_{p,corr}$	5.39 ± 0.15

Table 4.
Amplitude V_p estimation of the received sine-sweep type signal analyzed by time domain, frequency domain, and cross-correlation method, for the primary and secondary frequencies (parametric signal).

signal arrives. In contrast, a sine-type signal has only one frequency, which might easily be confused with background noise, and its correlation produces a wider and less defined peak, which makes it difficult to precisely identify the time of arrival.

The results of this second approach proposed in this chapter, related to the amplitude estimation, for the primary and secondary frequencies are shown in **Table 4**.

Using this type of parametric signal, it is possible to design a communication system based on binary coding, where bit 1 and bit 0 are represented, e.g., by ascending and descending sine-sweep signals, respectively. It is important to note that other types of modulated signals are also capable of generating this parametric effect, potentially enabling their use in binary transmission schemes [23, 24]. This approach offers a significant advantage by exploiting the properties of low-frequency nonlinear signals, as they can travel much longer distances due to lower absorption by the medium, unlike high-frequency signals that experience greater attenuation. Despite its lower frequency, the nonlinear signal can maintain a narrow directivity similar to that of high frequency signals. This property enables the signal to be focused with high precision on a specific receiver, facilitating communication over long distances without the signal being picked up by other sensors in the same environment. This allows for efficient and targeted transmission, ideal for scenarios where interference minimization and long-range coverage are key factors.

7. Conclusion

In this chapter, the parametric effect of low frequencies has been presented in a controlled environment as a proof of concept. The phenomenon was demonstrated experimentally using both sine-type and sine-sweep signals. Further research is needed to expand the understanding of this type of communication and to evaluate its performance in real environments over longer distances. This would support the optimization of a low-frequency, focused-beam bit transmission system.

The results presented indicate that threshold and Pvar methods for ToA estimation are highly sensitive to the SNR and the temporal slope of the input signal. These methods yield accurate estimates when the signal exhibits abrupt transitions such as in sine signals waveforms, but their performance deteriorates significantly in the presence of gradual transitions, as seen in sine-sweep signals. This strong dependence on signal morphology limits their applicability in scenarios where the temporal profile of

the signal cannot be precisely controlled or predicted. By contrast, the cross-correlation method demonstrates superior robustness to temporal variations, delivering more consistent and accurate ToA estimates. Nevertheless, its effectiveness relies on the availability of a reference signal for correlation, which restricts its use in passive detection contexts or in the analysis of acoustic signals of unknown origin, as frequently encountered in bioacoustic applications.

Regarding to amplitude V_p estimation, the nonuniform spectral content of sine-sweep type signals, compounded by the nonlinear frequency response of the sensor, particularly at higher frequencies, poses significant challenges for accurate estimation using conventional time domain methods. Specifically, these methods require both a high SNR and a temporally constant amplitude, conditions that are not fulfilled by weak parametric signals. As a result, alternative approaches based on frequency domain analysis and cross-correlation are employed, offering improved noise resilience and enabling more robust and reproducible amplitude estimation under demanding experimental conditions.

Acknowledgements

This work was a result of the ThinkInAzul and AgroAlNext programmes, funded by Ministerio de Ciencia, Innovación y Universidades (MICIU) with funding from European Union NextGenerationEU/PRTR-C17.I1 and by Fundación Séneca with funding from Comunidad Autónoma Región de Murcia (CARM).

Appendix

This workflow is not suitable for scenarios where the transmitter and receiver are separated by some of kilometers. At these distances, the secondary component of the signal tends to dominate, while the primary component is significantly attenuated, making it difficult, if not impossible, to accurately estimate the ToA. In such cases, although it is recognized that the accuracy of the ToA may be compromised, it is recommended to estimate it using correlation techniques applied to the secondary frequency (**Figure 11**).

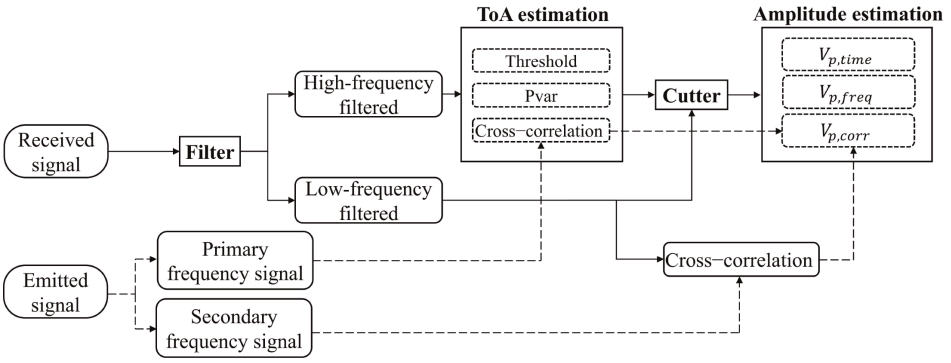

Figure 11.
Workflow summarizing the two proposed approaches: (i) ToA estimation, and (ii) amplitude estimation for nonlinear (parametric) signals, where a controlled system receives both primary (typically good SNR) and secondary (parametric) frequency components.

Author details

María Campo-Valera[1*†], Dídac Diego-Tortosa[2†] and Rafael Asorey-Cacheda[3,4]

1 Telecommunication Research Institute (TELMA), Universidad de Málaga, Málaga, Spain

2 Laboratori Nazionali del Sud (LNS), Istituto Nazionale di Fisica Nucleare (INFN), Catania, Italy

3 Department of Information and Communication Technologies, Universidad Politécnica de Cartagena, Antigones Plaza del Hospital, Cartagena, Spain

4 People Oriented Smart Technologies Laboratory, European University of Technology, European Union

*Address all correspondence to: maria.campo@ic.uma.es

† These authors contributed equally.

References

[1] Mishachandar B, Vairamuthu S. An underwater cognitive acoustic network strategy for efficient spectrum utilization. Applied Acoustics. 2021;**175**: 107861. DOI: 10.1016/j.apacoust.2020.107861

[2] Diego-Tortosa D, Bonanno D, Bou-Cabo M, Di Mauro LS, Idrissi A, Lara G, et al. Effective strategies for automatic analysis of acoustic signals in long-term monitoring. Journal of Marine Science and Engineering. 2025;**13**(3):454. DOI: 10.3390/jmse13030454

[3] Guan S, Brookens T, Vignola J. Use of underwater acoustics in marine conservation and policy: Previous advances, current status, and future needs. Journal of Marine Science and Engineering. 2021;**9**(2):173. DOI: 10.3390/jmse9020173

[4] Aman W, Al-Kuwari S, Muzzammil M, Rahman MMU, Kumar A. Security of underwater and air–water wireless communication: State-of-the-art, challenges and outlook. Ad Hoc Networks. 2023;**142**:103114. DOI: 10.1016/j.adhoc.2023.103114

[5] Westervelt PJ. Parametric acoustic array. The Journal of the Acoustical Society of America. 1963;**35**(4):535-537. DOI: 10.1121/1.1918525

[6] Berktay HO. Possible exploitation of non-linear acoustics in underwater transmitting applications. Journal of Sound and Vibration. 1965;**2**(4):435-461. DOI: 10.1016/0022-460X(65)90122-7

[7] López-Fernández J, Fernández-Plazaola U, Paris JF, Díez L, Martos-Naya E. Wideband ultrasonic acoustic underwater channels: Measurements and characterization. IEEE Transactions on Vehicular Technology. 2020;**69**(4): 4019-4032. DOI: 10.1109/TVT.2020.2973495

[8] Gunes A. Performance comparison of toa and tdoa based tracking in underwater multipath environments using bernoulli filter. Polish Maritime Research. 2023;**30**(1):135-144. DOI: 10.2478/pomr-2023-0014

[9] Li X, Chen J, Bai J, Ayub MS, Zhang D, Wang M, et al. Deep learning-based doa estimation using crnn for underwater acoustic arrays. Frontiers in Marine Science. 2022;**9**:1027830. DOI: 10.3389/fmars.2022.1027830

[10] Gao R, Liang M, Dong H, Luo X, Suganthan PN. Underwater acoustic signal denoising algorithms: A survey of the state-of-the-art. IEEE Transactions on Instrumentation and Measurement. 2025;**74**:6502318

[11] Campo-Valera M, Diego-Tortosa D, Rodríguez-Rodríguez I, Useche-Ramírez J, Asorey-Cacheda R. Signal processing to characterize and evaluate nonlinear acoustic signals applied to underwater communications. Electronics. 2024;**13**(21):4192. DOI: 10.3390/electronics13214192

[12] Tjo/tta JN, Tjo/tta S. Nonlinear equations of acoustics, with application to parametric acoustic arrays. The Journal of the Acoustical Society of America. 1981;**69**(6):1644-1652. DOI: 10.1121/1.385942

[13] Enflo BO, Hedberg CM. Theory of Nonlinear Acoustics in Fluids. Vol. 67. Netherlands: Springer; 2006. ISBN 978-0-306-48419-3

[14] Campo-Valera M, Felis I. Underwater acoustic communication for

the marine enviroment's monitoring. In: MDPI Proceedings, (ECSA-6) 6th International Elecctronic Conference on Sensors and Applications. Vol. 42(51). Switzerland: MDPI; 2019

[15] Campo-Valera M, Villó-Pérez I, Fernández-Garrido A, Rodríguez-Rodríguez I, Asorey-Cacheda R. Exploring the parametric effect in nonlinear acoustic waves. IEEE Access. 2023;**11**:97221-97238. DOI: 10.1109/ACCESS.2023.3311631

[16] Oppenheim AV, Schafer RW. Tratamiento de señales en tiempo discreto. Old Tappan, N.J: Prentice Hall; 2011

[17] Youn D, Mathews V. Adaptive realizations of the maximum likelihood processor for time delay estimation. IEEE Transactions on Acoustics, Speech, and Signal Processing. 1984;**32**(4): 938-940. DOI: 10.1109/TASSP.1984.1164407

[18] Proakis JG. Digital Signal Processing: Principles Algorithms and Applications. Upper Saddle River, NJ, United States: Prentice-Hall, Inc. Division of Simon and Schuster; 1996. ISBN: 978-0-13-373762-2

[19] Cabot R. A note on the application of the hilbert transform to time delay estimation. IEEE Transactions on Acoustics, Speech, and Signal Processing. 1981;**29**(3):607-609. DOI: 10.1109/TASSP.1981.1163564

[20] Choi H-I, Williams WJ. Improved time-frequency representation of multicomponent signals using exponential kernels. IEEE Transactions on Acoustics, Speech, and Signal Processing. 1989;**37**(6):862-871. DOI: 10.1109/assp.1989.28057. ISSN 0096-3518

[21] Serrano EGF, Cardona S, i Foix, and Lluisa Jordi Nebot. Análisis en tiempo y frecuencia de señales de vibración tomadas al pie del carril durante el paso de un tren. Scientia et Technica. 2007; **13**(35):243-247. ISSN 0122-1701

[22] Adrián-Martínez S, Bou-Cabo M, Felis I, Llorens CD, Martínez-Mora JA, Saldaña M, et al. Acoustic Signal Detection through the Cross-Correlation Method in Experiments with Different Signal to Noise Ratio and Reverberation Conditions. Berlin Heidelberg: Springer; 2015. pp. 66-79. DOI: 10.1007/978-3-662-46338-3_7

[23] Campo-Valera M, Felis-Enguix I, Villó-Pérez I. Signal processing for parametric acoustic sources applied to underwater communication. Sensors. 2020;**20**(20):5878. DOI: 10.3390/s20205878. ISSN 1424-8220

[24] Campo-Valera M, Rodríguez-Rodríguez I, Rodríguez J-V, Herrera-Fernández L-J. Proof of concept of the use of the parametric effect in two media with application to underwater acoustic communications. Electronics. 2023;**12**(16):3459. DOI: 10.3390/electronics12163459